

1 **Hydrological and ecological changes in Western Europe between 3200**
2 **and 2000 years BP derived from lipid biomarker δD values in Lake**
3 **Meerfelder Maar sediments**

4
5
6 O. Rach^{1,2*}, S. Engels³, A. Kahmen⁴, A. Brauer⁵, C. Martín-Puertas^{5,6}, B. van
7 Geel⁷, D. Sachse¹

8
9 ¹GFZ German Research Centre for Geosciences, Section 5.1,
10 Geomorphology, Organic Surface Geochemistry Lab, Telegrafenberg, D-
11 14473 Potsdam, Germany

12 ²Institute for Earth- and Environmental Science, University of Potsdam, Karl-
13 Liebknecht-Strasse 24-25, 14476 Potsdam (Germany)

14 ³Centre for Environmental Geochemistry, School of Geography, University of
15 Nottingham, University Park, Nottingham (UK)

16 ⁴Botany – Department of Environmental Sciences, University of Basel,
17 Schönbeinstrasse 6, 4056 Basel (Switzerland)

18 ⁵GFZ German Research Centre for Geosciences, Section 5.2 Climate
19 Dynamics and Landscape Evolution, Telegrafenberg, 14473 Potsdam
20 (Germany)

21 ⁶Department of Geography, Royal Holloway, University of London, Egham,
22 Surrey TW20 0EX, United Kingdom.

23 ⁷Institute for Biodiversity and Ecosystem Dynamics, University of Amsterdam,
24 Science Park 904, 1098 XH Amsterdam (Netherlands)

25
26 * Corresponding author's email address: oliver.rach@gfz-potsdam.de
27
28

29 **Highlights**

- 30 - We present a high-resolution late Holocene biomarker δD record from
31 W Europe

- 32 - Terrestrial biomarker δD_{terr} records minor hydrological changes
33 between 3.2-2.0 cal ka BP
34 - δD_{terr} data are in agreement with other paleoecological data
35 - We observe significant effects of aquatic lipid source changes on the
36 δD_{aq} record
37 - Multiproxy approaches are essential to avoid hydrological
38 misinterpretations
39
40

41 **Keywords**

42 Holocene; Climate dynamics; Paleoclimatology; Western Europe; Continental
43 biomarkers; Organic geochemistry; Stable isotopes; Vegetation dynamics
44
45
46

47 **Abstract**

48 One of the most significant Late Holocene climate shifts occurred around
49 2800 years ago, when cooler and wetter climate conditions established in
50 western Europe. This shift coincided with an abrupt change in regional
51 atmospheric circulation between 2760 and 2560 cal years BP, which has
52 been linked to a grand solar minimum with the same duration (the Homeric
53 Minimum). We investigated the temporal sequence of hydroclimatic and
54 vegetation changes across this interval of climatic change (Homeric climate
55 oscillation) by using lipid biomarker stable hydrogen isotope ratios (δD values)
56 and pollen assemblages from the annually-laminated sediment record from
57 lake Meerfelder Maar (Germany).

58 Over the investigated interval (3200 to 2000 varve years BP), terrestrial lipid
59 biomarker δD showed a gradual trend to more negative values, consistent
60 with the western Europe long-term climate trend of the Late Holocene. At ca.
61 2640 varve years BP we identified a strong increase in aquatic plants and
62 algal remains, indicating a rapid change in the aquatic ecosystem
63 superimposed on this long-term trend. Interestingly, this aquatic ecosystem

64 change was accompanied by large changes in δD values of aquatic lipid
65 biomarkers, such as nC_{21} and nC_{23} (by between 22-30‰). As these variations
66 cannot solely be explained by hydroclimate changes, we suggest that these
67 changes in the δD_{aq} value were influenced by changes in *n*-alkane source
68 organisms. Our results illustrate that if ubiquitous aquatic lipid biomarkers are
69 derived from a limited pool of organisms, changes in lake ecology can be a
70 driving factor for variations on sedimentary lipid δD_{aq} values, which then could
71 be easily misinterpreted in terms of hydroclimatic changes.

72

73

74 **1. Introduction**

75 Late Holocene climate was characterized by a gradual long-term cooling trend
76 recognized globally (Marcott et al., 2013; Wanner et al., 2008), but also by
77 superimposed short-term climatic variations occurring over the lifetime of a
78 few generations and with strong impact on regional climate and society. For
79 example, a relatively abrupt cooling and increased humidity 2800 years ago in
80 the North Atlantic-European region (Swierczynski et al., 2013; Wirth et al.,
81 2013) were interpreted from peat bog records in the Netherlands (van Geel et
82 al., 1996; van Geel et al., 1999), glacial advances, and increased lake levels
83 throughout Europe (e.g. Magny, 1993; Engels et al., 2016a). This change
84 (Movius, 2013) coincided with a significant shift in the western Europe
85 landscape that marked the onset of the Subatlantic period (Litt et al., 2001).
86 The climate change 2800 years ago has been related to the occurrence of a
87 grand solar minimum (Magny, 1993; Martin-Puertas et al., 2012b; van Geel et
88 al., 1996; van Geel et al., 1999), the Homeric Minimum, which occurred
89 between 2750-2550 cal years BP recognized in both ^{14}C -tree rings (Reimer et
90 al., 2009) and ^{10}Be -Greenland ice core records (Reimer et al., 2009; Vonmoos
91 et al., 2006). Martin-Puertas et al. (2012b) recently reconstructed changes in
92 solar variability during the time interval from 3300 to 2000 years BP by
93 analyzing changes in ^{10}Be accumulation rates in the annually laminated
94 (varved) sediment record of lake Meerfelder Maar (MFM). The authors
95 compared the reconstructed changes in solar variability to changes in

96 windiness (reconstructed from varve thickness) using the sediment record.
97 The study showed a sharp increase (over less than a decade) in both the
98 climatic and solar proxies at 2759 ± 39 varve years BP and a reduction $199 \pm$
99 9 years later, indicating that atmospheric circulation reacted abruptly and in
100 phase with the grand solar minimum and hence showing empirical evidence
101 for a solar-induced “Homeric Climate Oscillation” (HCO).
102 The HCO has been suggested to be the trigger for human migrations during
103 the transition from Bronze Age to Iron Age (Scott et al., 2006; van Geel et al.,
104 1996). Archeological and paleoecological studies from different locations in
105 Europe (e.g. the Netherlands and Germany) also provide evidence for an
106 increase in human activity and reorganization of prehistoric cultures around
107 that time (Kubitz, 2000; van Geel et al., 1996), most likely favored by a rise in
108 human population density after the climate deterioration (van Geel and
109 Berglund, 2000). Although wetter conditions have been inferred for the HCO,
110 it yet remains elusive if these wetter conditions were associated to major
111 changes in rainfall intensity and/or lower evapotranspiration and the possible
112 relation to the observed vegetation changes in western Europe. Furthermore,
113 the exact temporal succession of regional hydrological and environmental
114 changes during this period is unknown due to the lack of highly-resolved
115 hydrological records in western Europe.
116 In this study we analyze high-resolution lipid biomarker hydrogen isotope
117 ratios of a Late Holocene sedimentary sequence from lake MFM in western
118 Germany to test its potential for elucidating the nature of hydrological changes
119 during the HCO. Stable hydrogen isotope ratios (expressed δD values) of
120 sedimentary lipid biomarkers (i.e. *n*-alkanes), which can be traced back to
121 their biological sources (Eglinton and Eglinton, 2008; Killups, 2005; Peters et
122 al., 2007; Sachs et al., 2013), have become an important paleohydrological
123 proxy over the last ca. 15 years. This has resulted in new insights into
124 hydroclimate dynamics over different geological timescales (Aichner et al.,
125 2010; Atwood and Sachs, 2014; Feakins et al., 2014; Rach et al., 2014;
126 Sachs et al., 2009; Schefuss et al., 2011; Smittenberg et al., 2011; Tierney et
127 al., 2010; Tierney et al., 2008; Zhang et al., 2014). Rach et al. (2014)

128 demonstrated that *n*-alkane δD analyzes are a suitable proxy for
129 reconstructing regional hydrological changes during major and abrupt climate
130 shifts during the Late-Glacial that are recorded in the varved sediments of lake
131 MFM.

132 Our specific objectives for this study are (1) to reconstruct hydroclimate
133 variations for central-western Europe during a period of changing
134 environmental conditions (3200-2000 varve years BP) using lipid biomarker
135 stable isotope data, and (2) to combine this record with a high-resolution
136 aquatic and terrestrial vegetation reconstruction in order to evaluate possible
137 effects of vegetation change on the biomarker stable isotope record.

138

139 **2. Lipid biomarkers as paleoclimate proxies**

140 *2.1 Sedimentary n-alkanes as biomarkers for aquatic and terrestrial* 141 *organisms*

142 Straight-chained hydrocarbons such as *n*-alkanes are increasingly applied for
143 paleoclimate reconstruction. Different *n*-alkane homologues are produced by
144 bacteria, aquatic as well as terrestrial plants (Aichner et al., 2010; Baas et al.,
145 2000; Cranwell et al., 1987; Eglinton and Hamilton, 1967; Ficken et al., 2000;
146 Gelpi et al., 1970). As such, *n*-alkanes can be used to obtain information on
147 their biological sources. While not species-specific, different groups of source
148 organisms can be distinguished based on *n*-alkane chain length: *n*-alkanes
149 with 17 to 19 (nC_{17} - nC_{19}) carbon atoms (short-chain) are predominantly
150 synthesized by aquatic algae but also by bacteria (Cranwell et al., 1987; Gelpi
151 et al., 1970; Sachse and Sachs, 2008). Mid-chain *n*-alkanes (nC_{21} - nC_{25}) are
152 mainly synthesized by submerged aquatic plants (Aichner et al., 2010; Baas
153 et al., 2000; Ficken et al., 2000). Long-chain *n*-alkanes (nC_{27} - nC_{31}) are major
154 components of the leaf waxes of terrestrial higher plants (Eglinton and
155 Hamilton, 1967; Massimo, 1996), although conifers produce significantly
156 smaller amounts of *n*-alkanes than broad-leaved species (Diefendorf et al.,
157 2011). Some terrestrial plants also produce significant amounts of nC_{25} ,
158 making source assessment for this compound more difficult, but in general

159 aquatic or terrestrial sources can be distinguished from *n*-alkane abundances
160 in sediments (Gao et al., 2011).

161

162 *2.2. Climatic and environmental influences on δD values of aquatic and* 163 *terrestrial biomarkers*

164 The observation that δD values of aquatic (δD_{aq}) and terrestrial (δD_{terr}) plant
165 derived lipid biomarkers record the δD values of the organisms' source water
166 (Garcin et al., 2012; Huang et al., 2004; Sachse et al., 2012; Sachse et al.,
167 2004; Sauer et al., 2001) has fueled the application of δD measurements as a
168 paleohydrological proxy. The major determinant of the δD values of aquatic
169 and terrestrial lipid biomarkers is the δD value of the source water used by the
170 organism (Sachse et al., 2012). Photosynthetic lacustrine aquatic organisms,
171 such as submerged aquatic macrophytes and algae use lake water as a
172 hydrogen source to synthesize *n*-alkanes. In a closed lake system (in
173 temperate climates), which is only fed by precipitation and characterized by a
174 low precipitation/ evaporation ratio, the hydrogen isotope composition of lake
175 water can be interpreted as an integrated signal of precipitation δD (Aichner
176 et al., 2010; Sachse et al., 2012). In particular, for MFM, being a maar with
177 steep catchment walls (sheltered from the wind) an effect of evaporation on
178 lake water is unlikely. For a neighboring maar lake (Holzmaar) a long-term
179 study of lake water has shown that $\delta^{18}O$ values vary only around 1‰ and
180 follow the seasonal temperature evolution (Moschen et al., 2005). Thus, in
181 such a lake system sedimentary δD_{aq} values provide an integrated
182 precipitation δD signal (Sachse et al., 2004).

183 Higher land plants on the other hand directly take up precipitation water
184 (through soil water) (Sachse et al., 2012). However, transpirative processes in
185 the leaf of the plant modify the isotopic composition of water (i.e. increased
186 enrichment in D under drier conditions) before hydrogen is being fed into
187 biosynthetic reactions (Kahmen et al., 2013a; Kahmen et al., 2013b; Sachse
188 et al., 2012). As a consequence, sedimentary δD_{terr} values also record
189 changes in ecosystem evapotranspiration (Kahmen et al., 2013b; Sachse et
190 al., 2004).

191

192 *2.3. Species-specific differences and their influence on aquatic and terrestrial*
193 *lipid δD values*

194 In addition to the isotopic composition of source water, it has been
195 demonstrated that changes in vegetation type (of terrestrial plants) as well as
196 aquatic lipid source organisms can also significantly affect the isotope
197 composition of terrestrial and aquatic lipids (Sachse et al., 2012).
198 For example, major differences in the net or apparent fractionation ($\epsilon_{l/w}$), i.e.
199 the isotopic difference between the source water (δD_w) and lipid (δD_l) (equ. 1),
200 have been observed among different plant functional types (Gao et al., 2014;
201 Sachse et al., 2012).

202

$$(1) \quad \epsilon_{l/w} = \frac{(D/H)_l}{(D/H)_w}$$

203

204 Since $\epsilon_{l/w}$ represents the sum of physical and biochemical fractionation
205 processes, it is currently unclear to what extent individual parameters are
206 responsible for the observed differences. For example, major differences in
207 the biosynthetic fractionation (ϵ_{bio}) between various species as well as
208 differences in leaf-morphology, transpiration and water use efficiency between
209 grasses and broadleaf-woody plants have been shown to affect $\epsilon_{l/w}$ (Kahmen
210 et al., 2013b; Liu et al., 2006; McInerney et al., 2011; Sachse et al., 2012).
211 On the other hand, $\epsilon_{l/w}$ in aquatic algae and cyanobacteria can also be
212 influenced by water salinity and growth rate, possibly related to biochemical
213 processes as shown for *n*-alkanoic acids (Sachs, 2014), the biosynthetic
214 precursors of *n*-alkanes (Eglinton and Eglinton, 2008; Sachse et al., 2012;
215 Sessions et al., 1999). In addition, significant differences in ϵ_{bio} have been
216 observed among different algae (Zhang and Sachs, 2007). For example,
217 under similar conditions in batch cultures, two different groups of green algae
218 (Chlorophyceae and Trebouxiophyceae) produced C_{16} *n*-alkanoic acids, which
219 differed in their δD values by 160‰ (Zhang and Sachs, 2007). Less
220 information is available for submerged aquatic plants, but studies on modern

221 aquatic plants and lake surface sediments have suggested the ϵ_{bio} for aquatic
222 macrophytes (i.e. *Potamogeton*) may be significantly smaller (-82‰) (Aichner
223 et al., 2010) than observed for algae (-157‰) (Sachse et al., 2004).
224 Therefore, if various algae and other water plants produce the same
225 unspecific biomarker (e.g. short- to mid-chain *n*-alkanes) and the aquatic
226 ecosystem (i.e. species composition) changes, the sedimentary *n*-alkane δD
227 record could be affected. In a similar way, major vegetation changes can
228 affect the $\delta\text{D}_{\text{terr}}$ signal (Nelson et al., 2013). Despite these complications, δD
229 values of aquatic and terrestrial lipids from sedimentary archives can be used
230 to reconstruct changes in hydroclimate over time, if constraints on the
231 processes discussed above, i.e. information about the terrestrial and aquatic
232 producers of the studied lipids, are available (Aichner et al., 2010; Atwood and
233 Sachs, 2014; Rach et al., 2014).

234

235 Therefore, for a robust paleoclimatic interpretation it is important to
236 understand the interplay between hydrological and vegetation change and
237 their effect on sedimentary lipid biomarker δD records. The here studied time
238 interval was characterized by long and short-term climatic change as well as
239 vegetation changes and this provides a testing ground to study the above
240 discussed processes and their influence on biomarker δD values. Therefore,
241 we compare a high-resolution $\delta\text{D}_{\text{aq}}$ and $\delta\text{D}_{\text{terr}}$ record from lake MFM in
242 western Germany to lake and catchment ecosystem development, inferred
243 from a new pollen-based vegetation reconstruction, as well as published
244 sedimentary proxy data from MFM, such as varve thickness and Ti influx
245 (Martin-Puertas et al., 2012b).

246

247 **3. Study site**

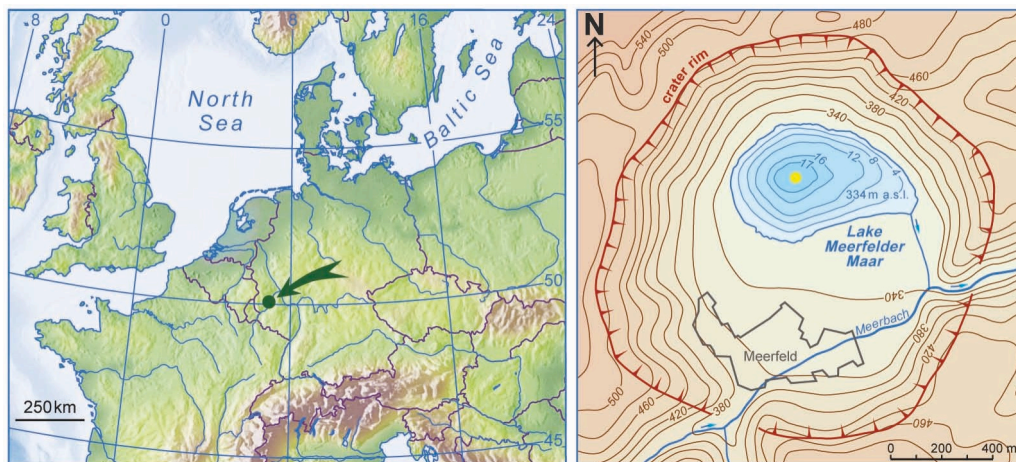
248 Lake Meerfelder Maar ($50^{\circ} 06' 2.87'' \text{ N}$; $06^{\circ} 45' 27.13'' \text{ E}$) is located in
249 western Germany as a part of the West-Eifel Volcanic Field (Fig. 1). The lake
250 is situated in a volcanic crater which was formed by a phreatomagmatic
251 eruption 80,000 years ago (Zöller, 2009).

252 The modern lake is situated at 336.5 m a.s.l. and the lake surface is around
253 0.248 km², covering the northern part (ca. 1/3) of the maar crater surface (Fig.
254 1). The maximum water depth is 18m. The southern part of the crater is filled
255 in by a shallow delta plain, deposited from a stream (Meerbach) passing
256 through the crater rim in the south. The lake is eutrophic and due to its
257 particular morphological situation within a deep maar crater, Lake MFM is
258 wind-sheltered, favoring the preservation of fine seasonal layers within the
259 sediment sequence (Brauer et al., 1999a; Brauer et al., 2008).

260 The climate of the region is influenced by its proximity to the North Sea coast
261 (ca. 250 km) with a mean annual air temperature of 8.2 °C and mean annual
262 precipitation of 950 mm, peaking in winter (Martin-Puertas et al., 2012a).

263 Seven sediment cores were collected in 2009 from the deepest area of Lake
264 MFM using a UWITEC piston core, with a maximum distance between sites of
265 20 m. The sediment cores, labeled as MFM09-A to MFM09-G, were split,
266 imaged, described and an overlapping sediment profile was constructed
267 (Martin-Puertas et al., 2012a). For the present study the uppermost core
268 MFM09-A was selected for sampling. We studied a meter long sequence from
269 230 to 330 cm depth, which covers the interval from 2000 to 3200 varve years
270 BP (Martin-Puertas et al., 2012b). The MFM chronology (MFM2000) has been
271 established by varve counting from ca. 1500 cal years BP back to 14,200 cal
272 years BP along 7.85 m of sediments with a cumulative counting error of less
273 than 5% and is supported by 51 radiocarbon dates (Brauer et al., 2000). This
274 independent but floating chronology was anchored to the calendar year time
275 scale by adopting the age of the regional (Eifel) Ulmener Maar Tephra (UMT)
276 for the MFM record (Brauer et al., 1999b; Brauer et al., 2000). The UMT is
277 dated at 11,000 ± 110 cal years BP in the Lake Holzmaar (HZM) varve
278 chronology by multiple count sequences and ¹⁴C based-correction (Zolitschka
279 et al., 2000). The proximity of Lake HZM to MFM (10 km) provides the
280 opportunity to compare both records, showing a good agreement between the
281 chronologies (Litt et al., 2009). For the study interval, an age error estimate
282 has been provided by combining varve counting, radiocarbon dating and
283 sediment ¹⁰Be accumulation rates (Martin-Puertas et al., 2012b). All ages in

284 the following text are rounded on 5 years to avoid interpretations on a
285 temporal accuracy level, which is not supported by the current age model.



286
287 **Fig. 1:** Map of western Europe with the study locations. Coloured dots mark
288 the study (left) and coring (right) site at MFM.

289

290 4. Methods

291 4.1 Biomarker extraction, identification and quantification

292 A 1.0-m-long core section, which included the time interval of the HCO, was
293 sampled in consecutive 1-cm-thick slices, resulting in a total of 100 samples.
294 Due to differences in sedimentation rate, the temporal resolution of the
295 samples varies between 4 and 45 years per sample.

296 To remove remaining water, all samples were freeze-dried and subsequently
297 homogenized. A Dionex accelerated solvent extraction system (ASE 350) with
298 a dichloromethane (DCM): methanol mixture (9:1) at 100°C and 103 bar was
299 used for the extraction of lipid biomarkers from freeze-dried samples in the
300 biomarker laboratory at the University of Potsdam. The total lipid extracts
301 (TLE) were separated into three fractions (aliphatic (F1), aromatic (F2) and
302 alcohol/ fatty acid (F3)) by solid phase extraction (SPE). The separation was
303 achieved using 2g silica gel as the stationary phase and hexane,
304 hexane:DCM (1:1) and DCM as the respective mobile phases. Activated
305 copper in a pipette column was used to remove elemental sulfur from the F1
306 fraction. The aliphatic fraction was dominated by *n*-alkanes (nC_{21} - nC_{31}
307 homologues) and alkenes. Fractions F2 and F3 contained mainly ketones,
308 alcohols and fatty acids. To avoid coelution of alkanes and alkenes during

309 isotope measurement, the F1 fraction was further purified using silver nitrate
310 (AgNO_3) impregnated silica gel in a pipette column with hexane and
311 dichloromethane as the mobile phase for the elution of alkanes and alkenes,
312 respectively.

313 *n*-Alkane identification and quantification was performed using a gas
314 chromatograph (GC 7890-A, Agilent, Santa Clara, USA) coupled to a flame
315 ionization detector (FID) and a mass selective detector (MSD) (MS 5975-C,
316 Agilent, Santa Clara, USA) coupled via an electronic split interface. The
317 quantification was performed through the FID by comparing compound peak
318 area to the peak area of the internal standard (5 α -androstane). Compound
319 identification was achieved using the MSD and comparison with library and
320 literature mass spectra. The GC temperature program used for *n*-alkane
321 quantification contained the following specifications: injection at 70°C (hold for
322 2 minutes), then heating up to 140°C with a ramp of 12°C per minute directly
323 followed by a heating to 320°C with a ramp of 2°C per minute. The final
324 temperature of 320°C was held for 15 minutes. The PTV injector started at
325 50°C and was heating up to 350°C with a ramp of 14°C per second.

326

327 *4.2 Stable isotope measurement and evaluation*

328 Compound-specific hydrogen isotope ratios of the *n*-alkanes were measured
329 on a Delta-V-Plus Isotope Ratio Mass Spectrometer (IRMS) (Thermo Fisher,
330 Bremer, Germany) coupled to a Trace Gas Chromatograph Ultra (Thermo
331 Fisher, Bremer, Germany) at the Swiss Federal Institute of Technology Zurich
332 (ETH Zurich). The following GC-temperature program was used: start at 90°C
333 (held for 2 minutes), heating up to 150°C with 10°C per minute, heating from
334 150°C to 320°C with 4°C per minute; the final temperature was held for 10
335 minutes. Each sample was injected three times. For conversion of the
336 measured δD values to the VSMOW scale a standard containing $n\text{C}_{16}$ to $n\text{C}_{30}$
337 alkanes (Mix A4 obtained from Arndt Schimmelmann, Indiana University) with
338 known δD values was measured in triplicate at the beginning and the end of
339 each sequence. All measured δD values were corrected to the VSMOW scale
340 using a linear regression function (with a specific slope and intercept) derived

341 from measured vs. real Mix A4 standard values. The mean standard deviation
342 of all A4 standard measurements (n=441) was 2.1‰, while the mean
343 standard deviation of all sample *n*-alkane measurements (n=492) was 1.4‰.
344 To avoid misinterpretation of the measured δD values only baseline separated
345 peaks with areas over 20V have been used for interpretation. The H3⁺ factor
346 was determined before each sequence and remained constant at 3.63 ± 0.39
347 during the 4 weeks measurement period.

348

349 *4.3 Palynological analysis*

350 Two plastic containers of 35x260 mm were pressed into cores MFM09A2DR
351 and MFM09A2UR to a depth of 10 mm. The sediment in the plastic containers
352 was subsequently subsampled with a 3 samples/ centimeter resolution for the
353 sediments older than 2765 varve years BP and a 2 samples/ centimeter
354 resolution for the sediments younger than 2765 varve years BP. These
355 sampling intervals correspond to a temporal resolution of 1-29 years per
356 sample. Ninety-one samples were prepared for the analysis of pollen and
357 spores at the University of Amsterdam following the protocols of Faegri et al.
358 (1990) and Moore et al. (1991). Standard tablets with *Lycopodium* spores
359 were added to the sample during laboratory processing to estimate pollen and
360 spore concentrations and influx numbers (Stockmarr, 1971). Pollen, fern
361 spores, fungal spores, and other palynomorphs (including remains of
362 freshwater algae) were identified using a light microscope with 400x
363 magnification (1000x when necessary). Keys and illustrations by Moore et al.
364 (1991) and Beug (2004) as well as a reference collection were used for pollen
365 identification. The identification of algal remains and other non-pollen
366 palynomorphs (NPPs) follows van Geel (1978). A pollen percentage diagram
367 was calculated using a pollen sum (Σ -pollen) that includes arboreal pollen and
368 pollen of upland herbs and the average Σ -pollen is 572 (range: 443-698). The
369 percent-abundances of all pollen, spores and NPPs are calculated in relation
370 to Σ -pollen. Concentrations of individual taxa were calculated by multiplying
371 the number of encountered pollen by the ratio of the number of added
372 *Lycopodium* spores and the number of spores encountered during analysis.

373 This number was then divided by the volume of material used in the analysis
374 to derive taxon-specific pollen concentrations. A percent-abundance diagram
375 was plotted using TILIA v 1.17.6; concentration- and influx-diagrams were
376 plotted using C2. Details on the taxa important for the interpretation of our *n*-
377 alkane data are presented in section 5.3 (pollen data), whereas overview
378 diagrams of the arboreal taxa (percentages, concentrations and influx) (Fig.
379 S1) and the aquatic taxa (expressed as percentages in relation to Σ -pollen)
380 (Fig. S2) can be found in the Supplementary Information.

381

382

383 5. Results

384 5.1 *n*-Alkane concentrations

385

386 In total 100 samples were analyzed for their *n*-alkane content. Eighteen
387 samples did not contain enough material for *n*-alkane analysis. In the
388 remaining 82 samples the concentration of all identified *n*-alkanes (nC_{21} to
389 nC_{31}) ranged from 0.34 to 69.42 $\mu\text{g/g}$ dry weight of sediment. The most
390 abundant *n*-alkane homologue in all samples was nC_{29} with an average
391 concentration of 26.5 $\mu\text{g/g}$ sediment dry weight per sample (range 3.0-
392 69.1 $\mu\text{g/g}$). The compound with the lowest concentration was always nC_{21} with
393 3.9 $\mu\text{g/g}$ on average (range 0.34 -14.3 $\mu\text{g/g}$). Other *n*-alkanes (nC_{23} , nC_{25} , nC_{27}
394 and nC_{31}) had average concentrations between 4.2 to 20.5 $\mu\text{g/g}$ sediment dry
395 weight. The average chain-length (ACL) varied between 26.0 and 28.8.

396 The average influx values (μg normalized per varve year) of short- and long-
397 chain *n*-alkanes showed significant variations. Before the HCO, nC_{21} and nC_{23}
398 showed average influx values of 0.35 and 0.27 $\mu\text{g/ year}$, while the nC_{25} to nC_{31}
399 homologues showed average influx values between 0.46 and 1.34 $\mu\text{g/year}$,
400 respectively (Fig 2B). The influx of nC_{21} and nC_{23} increased rapidly to 0.68
401 and 1.03 $\mu\text{g/ year}$ after 2785 varve years BP, while the influx values of nC_{25} to
402 nC_{31} also increased to average values between 2.10 and 6.28 $\mu\text{g/year}$ (Fig
403 2B). The average *n*-alkane influx values for nC_{21} and nC_{23} decreased abruptly
404 to average values of 0.12 and 0.15 $\mu\text{g/ year}$ after the HCO (Fig 2B). The nC_{25}

405 to nC_{31} homologues also decreased to average influx values between 0.37
406 and $1.42\mu\text{g}/\text{year}$. nC_{21} showed maximum influx values during the first part of
407 the HCO (2750 – 2660 varve years BP), while long-chain n -alkanes had their
408 maximum influx rates in the second part of the HCO (2700 – 2610 varve years
409 BP) (Fig 2B). Influx rates of nC_{23} showed local maxima both in the first half of
410 the HCO (at 2740 varve years BP) as well as in the second half of the HCO
411 (at 2610 varve years BP) (Fig 2B).

412

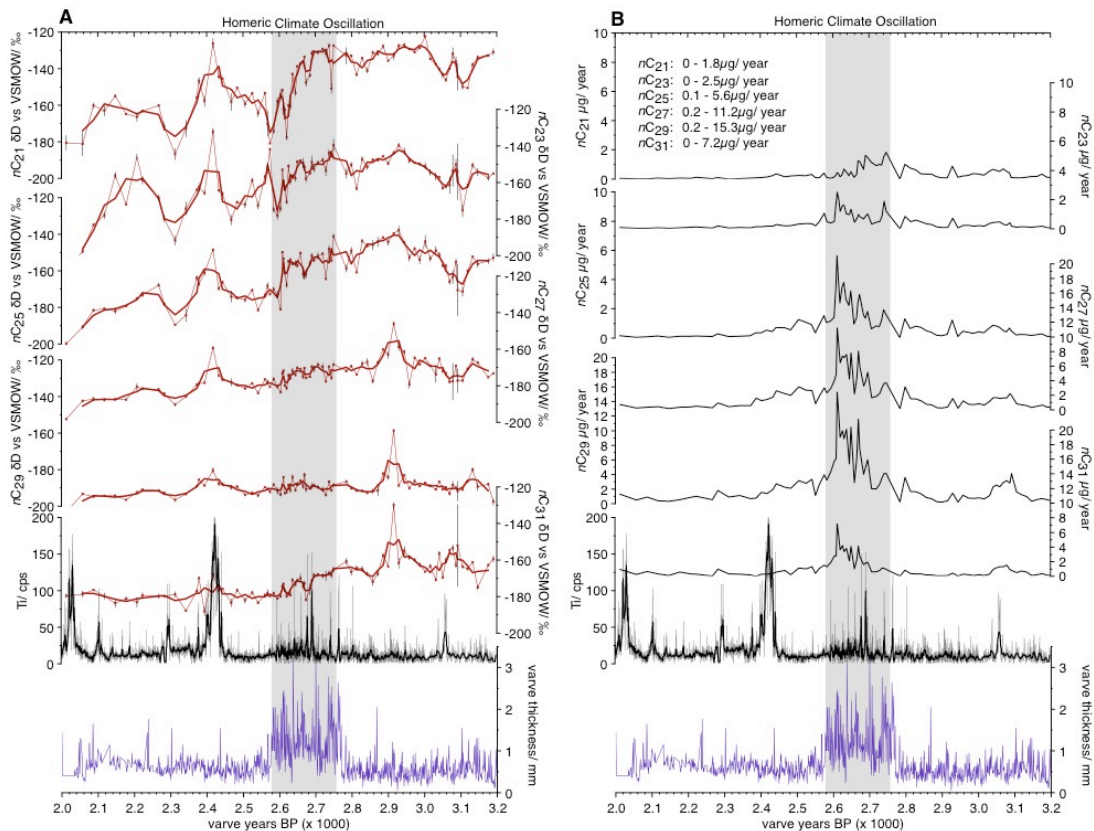
413 *5.2 Stable hydrogen isotope composition (δD values) of the n -alkanes*

414 All 82 samples were analyzed for compound specific stable hydrogen isotope
415 ratios, expressed as δD values. The n -alkane δD values showed a
416 decreasing trend during the analyzed period (Fig 2A). Generally, the δD
417 values of all n -alkanes were more positive before the HCO than after (Fig 2A).
418 However, there were major differences in the magnitude of variation between
419 n -alkanes of different chain-length. Short and mid-chain n -alkanes (nC_{21} - nC_{25})
420 generally showed higher variability in their δD values than long-chain n -
421 alkanes. Before the HCO, nC_{21} δD values were on average $-135 \pm 2\%$
422 (arithmetic mean from 3190 to 2785 varve years BP with respective 95%
423 confidence interval) while after the HCO the average δD value changed to -
424 $160 \pm 5\%$ (arithmetic mean from 2540 to 2015 varve years BP). Applying the
425 epsilon equation (Sessions and Hayes, 2005) for accurate calculations of
426 differences in δ -values results in a difference of about 30‰ for nC_{21} δD values
427 before and after the HCO. The average δD values of nC_{23} and nC_{25} for the
428 same period changed from $-153 \pm 3\%$ and $-152 \pm 3\%$ to $-171 \pm 7\%$ and -176
429 $\pm 4\%$, respectively (difference 22 and 28‰) (Fig 2A).

430 Long-chain n -alkanes generally showed smaller changes in their δD values.

431 The average δD values of nC_{27} and nC_{29} changed from $-169 \pm 2\%$ and $-188 \pm$
432 2% (before the HCO) to $-182 \pm 3\%$ and $-192 \pm 2\%$ (after the HCO) (difference
433 15 and 4‰). The δD values of nC_{31} changed from $-162 \pm 3\%$ to $-179 \pm 2\%$
434 (difference 20‰) (Fig 2A).

435



436

437 **Fig. 2:** δD values (A) (smoothing by 3-data running average) and annual flux
 438 ($\mu\text{g}/\text{year}$) (B) of nC_{21} - nC_{31} alkanes and varve thickness as well as Titanium
 439 content (smoothing by 100-data running average) (Martin-Puertas et al.,
 440 2012b) of the studied core section.

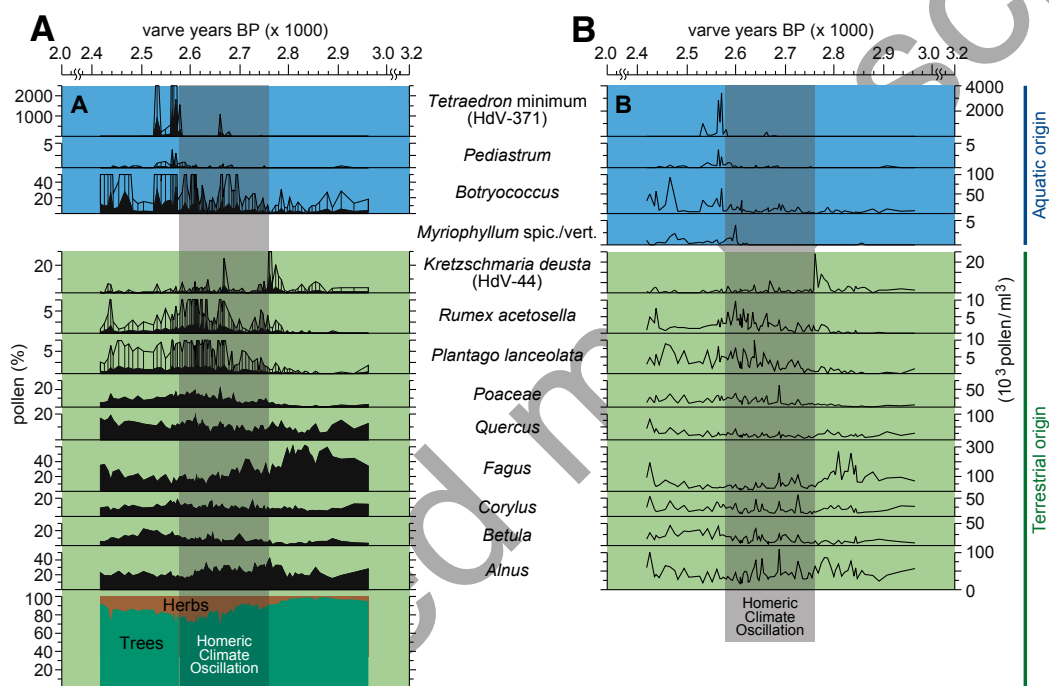
441

442 5.3 Pollen-data

443 The lower part of the pollen record (2945-2795 varve years BP) was
 444 characterized by relatively high percentages of arboreal pollen (AP) of 95-
 445 100% (Fig. 3). The pollen-assemblages were dominated by *Fagus* which
 446 reached abundances $>60\%$, accompanied by relatively high abundances of
 447 other deciduous tree taxa such as *Alnus* (15-30%), *Corylus* (5-15%) and
 448 *Quercus* (5-15%). Pollen from non-arboreal taxa (NAP) were only present in
 449 low abundances between 2945-2795 varve years BP, suggesting that the
 450 vegetation around MFM consisted of a closed-canopy forest.

451 A sharp decrease in relative abundance of *Fagus* to values of around 40%
 452 was observed at ~ 2795 varve years BP (Fig. 3). Simultaneously, spores of
 453 *Kretzschmaria deusta*, a parasitic fungus living on various tree species (van

454 Geel et al., 2013), showed an increase in abundance to values of 5%. An
 455 increase in the relative abundance of *Alnus* as well as of several NAP-taxa
 456 coincided with the decrease in *Fagus* (Fig. 3). Crop plants (e.g. Poaceae,
 457 Cerealia) as well as *Plantago lanceolata* and *Rumex acetosella*-type all
 458 started to increase after 2795 varve years BP. Remains (vegetative cell walls)
 459 of the green algae *Botryococcus*, *Tetraedron minimum* and of the aquatic
 460 macrophyte *Myriophyllum spicatum/verticillatum*-type showed an increase
 461 around 2620 and 2595 varve years BP, respectively.
 462



463
 464 **Fig. 3:** Pollen and spores abundance of the major constituents of vegetation
 465 in and surrounding MFM given in % (A) and pollen concentrations (B). Thinner
 466 lines on top of the upper six plots in A marking exaggeration-lines (5-times).
 467 Blue shaded areas marking aquatic organisms. Green areas are showing
 468 terrestrial plants. The dark-green/ orange areas show the local tree/ herb
 469 distribution in percentage.

470

471 6. Discussion

472 Our lipid biomarker stable hydrogen isotope record showed a long-term trend
 473 to more negative δD values during the 3200 to 2000 varve years BP interval.
 474 This is evident in all analyzed biomarkers, regardless of their biological origin

475 (Fig. 2). The decrease in lipid δD values possibly reflects the long-term
476 cooling trend as a consequence of declining summer insolation in the
477 Northern Hemisphere (Marcott et al., 2013; Renssen et al., 2009) in the way
478 that a decrease in air temperature would lead to more negative precipitation
479 δD values (Dansgaard, 1964; Gat, 1996; Gat et al., 2000). However, we
480 observed substantial differences in the magnitude of changes in δD values
481 between aquatic and terrestrial plant derived lipid biomarkers: δD_{aq} values
482 showed a rather abrupt decrease starting at around 2700 varve years BP, a
483 change not observed for δD_{terr} values (except a slight decrease in nC_{31} δD
484 values). This indicates that different processes controlled the observed
485 changes for aquatic and terrestrial biomarkers. While different biosynthetic
486 fractionation factors for aquatic and terrestrial plants can explain different
487 absolute δD values, different magnitudes of change indicate either significant
488 evapotranspirational or ecological changes. For example, cooler and more
489 arid conditions could explain a stronger decrease in δD_{aq} compared to δD_{terr} ,
490 as δD_{terr} values would reflect increasing plant transpiration (Kahmen et al.,
491 2013b). However, there is no evidence for a substantial aridification during
492 this period in western Europe. Rather, several studies suggest a shift to more
493 humid conditions during this period (Martin-Puertas et al., 2012b; van Geel,
494 1978; van Geel et al., 1996; van Geel et al., 2013). With our combined high-
495 resolution lipid biomarker and palynological analysis we therefore explore
496 ecological changes in the aquatic and terrestrial ecosystem in and around
497 MFM to test if these changes may have influenced the magnitude of change
498 in biomarker δD values.

499

500 6.1. Changes in vegetation based on palynological records

501 The palynological data provide first evidence for changes in the terrestrial
502 ecosystem at ca. 2800 varve years BP. Our pollen record showed a decrease
503 in relative pollen abundance of *Fagus* by half and a doubling of *Alnus*,
504 accompanied by a general trend to increasing grass/herb vegetation in the
505 catchment of MFM (Fig. 3A). The presence/increase of human-impact
506 indicators such as *Plantago lanceolata* and *Rumex acetosella*-type provided

507 evidence for increased human impact (Behre, 1981) in the catchment of MFM.
508 *Kretzschmaria deusta* spores increased in abundance from 2795 to 2765
509 varve years BP, which could be a result of the temporary occurrence of this
510 fungus on wounded trees that were present in the landscape after the clearing
511 of parts of the forest (Kubitz, 2000; van Geel et al., 2013).

512 The second substantial decline in tree pollen at 2695 varve years BP occurred
513 about 100 years after the variations mentioned above (Fig 3A). This marks a
514 second phase of ecosystem changes, which is additionally characterized by
515 an increase of *Botryococcus* – green algae (Fig 3A). This second phase in
516 ecological change could even have been caused by further increased human
517 impact but climatic changes cannot be ruled out either.

518

519 *6.2. Environmental and hydroclimatic changes inferred from changes in lipid*
520 *biomarker abundance and δD values*

521

522 *6.2.1 Terrestrial biomarker flux into the sediment*

523 At 2695 varve years BP, about 60 years after the increase in varve thickness
524 (Fig 2) (Martin-Puertas et al., 2012b), our lipid biomarker record showed an
525 increased influx of leaf wax *n*-alkanes into the sediment (Fig 2B). This
526 doubling in lipid biomarker flux occurred simultaneous with an increase in
527 Titanium counts, a proxy for surface runoff (Fig. 2) (Martin-Puertas et al.,
528 2012b). At the same time, tree pollen decreased significantly (from 90-71%)
529 and grass and other herbaceous pollen increased from 10 to 29% (Fig. 3A).
530 We interpret these changes in the pollen record to reflect a shift toward a
531 more open landscape, which might have led to increased erosion and flux of
532 terrestrial material into the lake. This is supported by the observation that the
533 influx of terrestrial biomarkers reached its maximum at the same time when
534 the tree / herb pollen ratios showed their lowest value at ca. 2610 varve years
535 BP. However, the onset of the tree pollen decline (from 96-86%) and
536 increasing grass pollen (from 4 to 14%) occurred already 100 years earlier, at
537 ca. 2800 varve years BP. Also, varve thickness increased likely because of

538 windier conditions already ca. 60 years before the increased terrestrial lipid
539 biomarker influx at 2760 varve years BP.

540 The decadal resolution of our lipid biomarker and palynological data allows a
541 detailed assessment of the temporal succession of proxy changes related to
542 the HCO. We have to note that the different vegetation proxies presented here
543 (alkanes, pollen) partly may reflect different source areas. While most of the
544 *n*-alkanes likely were derived from vegetation growing on the lake shore,
545 pollen assemblages may also include a signal from the upland vegetation
546 surrounding the MFM crater. However, the specific catchment-conditions of
547 lake MFM, with its steep crater walls and small catchment area, make it most
548 likely that most pollen is derived from the catchment vegetation itself, and that
549 the contribution of long distance transport is of minor importance (Engels et
550 al., 2016b; Litt et al., 2009). The initial change in the pollen diagram observed
551 at ca. 2800 varve years BP is not linked to additional transport of terrestrial
552 material into the lake. Only at ca. 2700 varve years BP, when the largest
553 vegetation change occurred, soil erosion increased. The first decrease in
554 pollen concentrations at 2800 varve years BP may be due to decreased
555 pollen production as a result of increased ecological stress, instead of
556 changes in vegetation, which may have followed a few decades later.

557
558

559 *6.2.2 Biomarker δD values as recorders of hydroclimate*

560 In addition to the long-term trend to more negative δD values between 3200
561 and 2000 varve years BP (Fig. 2A), evident in nearly all analyzed biomarkers
562 (except *nC₂₉*), aquatic and terrestrial lipid biomarker δD values showed their
563 most substantial decrease (by between 30 and 4‰) during the HCO interval
564 (Fig. 4).

565 While the 4-20‰ decrease in δD_{terr} values could have been caused by a
566 combination of cooler conditions and lower plant transpiration (Craig, 1965;
567 Flanagan et al., 1991; Kahmen et al., 2013b; Sachse et al., 2012) under the
568 more humid conditions suggested by earlier studies (van Geel et al., 1996), it

569 remains difficult to explain the rapid decline in δD_{aq} values between 22-30‰,
570 as these would not be affected by changes in terrestrial transpiration.
571 While a decrease in air temperature would lead to more negative precipitation
572 δD values, the observed decrease of 22-30‰ in δD_{aq} would imply an
573 unrealistic temperature decrease between 11 and 15°C during the HCO, when
574 considering the modern temperature sensitivity of precipitation δD in this
575 region (2‰/°C; (IAEA/WMO, 2006)). While no temperature reconstructions
576 are available for the HCO, a temperature decrease between 0.5-1.5°C has
577 been suggested for similar solar minima (Martin-Puertas et al., 2012b).
578 Therefore, a potential 0.5-1.5°C decrease during the HCO would only have
579 had a minimal effect on precipitation δD values. However, a decrease in
580 temperature may also be associated to shifts in the moisture source region
581 and/or changes in moisture source temperature, which may have exercised
582 additional control on decreasing δD values. For example, Martin-Puertas et al.
583 (2012b) suggested a reduced atmospheric pressure gradient between the
584 subtropics and Iceland for the HCO, resembling a negative phase of the North
585 Atlantic Oscillation (NAO), which today results in more negative winter δD_{precip}
586 values in parts of western Europe (Baldini et al., 2008). However, we do not
587 observe an increase in δD values after the HCO, suggesting the observed
588 change was not an excursion or phase but rather a shift of atmospheric
589 conditions to a new regime.

590 While the relatively small changes in δD_{terr} can be largely explained by the
591 proposed long-term hydroclimatic changes during this period, the abrupt
592 changes in δD_{aq} of up to 30‰ over 180 years are difficult to reconcile with this
593 scenario. Due to the absence of other proxy indicators suggesting
594 hydroclimatic changes that could explain such a decline in δD_{aq} , we explore
595 the possibility that factors additional to hydroclimate influenced δD_{aq} .

596

597 *6.2.3. The effect of lake ecosystem changes on δD values of aquatic n-* 598 *alkanes*

599 Additional factors known to affect δD_{aq} include changes in water salinity, light
600 intensity, growth rate and species changes (Sachs, 2014; Zhang and Sachs,

2007). MFM always was a freshwater lake, so that we can rule out salinity as a driver. Increased upland erosion and a subsequent delivery of nutrients into the lake may have resulted in increasing growth rates of aquatic organisms. However, for aliphatic lipids produced by algae D/H fractionation does not seem to change significantly with growth rate (Sachs, 2014), and no such data exist for aquatic plants.

However, palynological data indicate significant changes in the aquatic ecosystem at 2625 varve years BP, when the total amount of aquatic and swamp taxa pollen/ remains started to increase from virtually zero to a maximum of 1.5% at 2600 varve years BP (Fig. 4). Strikingly, this increase, as well as the change in species composition, was synchronous to the largest changes in nC_{21} and nC_{23} alkane δD values (Fig 4). These compounds are primarily synthesized by aquatic organisms, likely aquatic macrophytes (Aichner et al., 2010; Cranwell et al., 1987). A minor decrease was also observed for nC_{25} δD (Fig 2) values, a compound that can originate from both aquatic as well as terrestrial sources (Baas et al., 2000; Eglinton and Hamilton, 1967; Ficken et al., 2000). Palynological analysis indicates the occurrence / increase of *Myriophyllum spicatum/verticillatum*-type (submerged aquatic plant), *Botryococcus*, *Pediastrum* and *Tetraedron minimum* (green algae) during and after the HCO (Fig. 3). The most abundant aquatic taxon identified from the microfossil record is *Botryococcus* (identified by vegetative cell walls). As such, the available palynological data indicate major changes in the aquatic ecosystem at 2625 varve years BP, coeval with the largest change in δD_{aq} values. Since nC_{21} and nC_{23} alkanes can be produced by a variety of different algae and submerged aquatic macrophytes (Aichner et al., 2010; Ficken et al., 2000; Gelpi et al., 1970; Parrish, 1988) it is possible that a change in the predominant aquatic organisms, characterized by different magnitudes of ϵ_{bio} , was at least partly responsible for the observed changes.

For the more ubiquitous nC_{16} alkanic acid differences in ϵ_{bio} of up to 160‰ between different green algal taxa have been observed in culture studies (Zhang and Sachs, 2007). As such, if the spectrum of organisms producing nC_{21} and nC_{23} was relatively small, which is supported by the limited number

633 of pollen of aquatic taxa (Fig 3), it is conceivable that changes in the
634 predominant nC_{21} and nC_{23} producers have resulted in a significant variation
635 within the sedimentary δD_{aq} record.

636 Therefore, we argue that the change in the δD values of the nC_{21} and nC_{23}
637 alkanes does not only reflect hydroclimatic changes, but that it was amplified
638 as a result of a change in aquatic lipid sources. This also implies that without
639 knowledge of the biosynthetic fractionation factors for the individual nC_{21} and
640 nC_{23} producers, a direct reconstruction of source water δD values is
641 impossible. Arguably, the observed changes in the aquatic ecosystem were
642 most probably initiated by the climatic and environmental changes. We
643 suggest that the increasing influx of terrestrial material between 2695 and
644 2610 varve years BP due to wetter conditions and decreasing tree cover (see
645 section 6.2.1), delivered more nutrients into the lake, acting as a fertilizer for
646 aquatic plants. The increase in abundance of aquatic organisms around 2640
647 varve years BP occurred 60 years after the increase of terrestrial biomarker
648 flux into the lake, possibly marking a threshold in the fertilization rate and
649 triggering the diversification of the aquatic ecosystem.

650

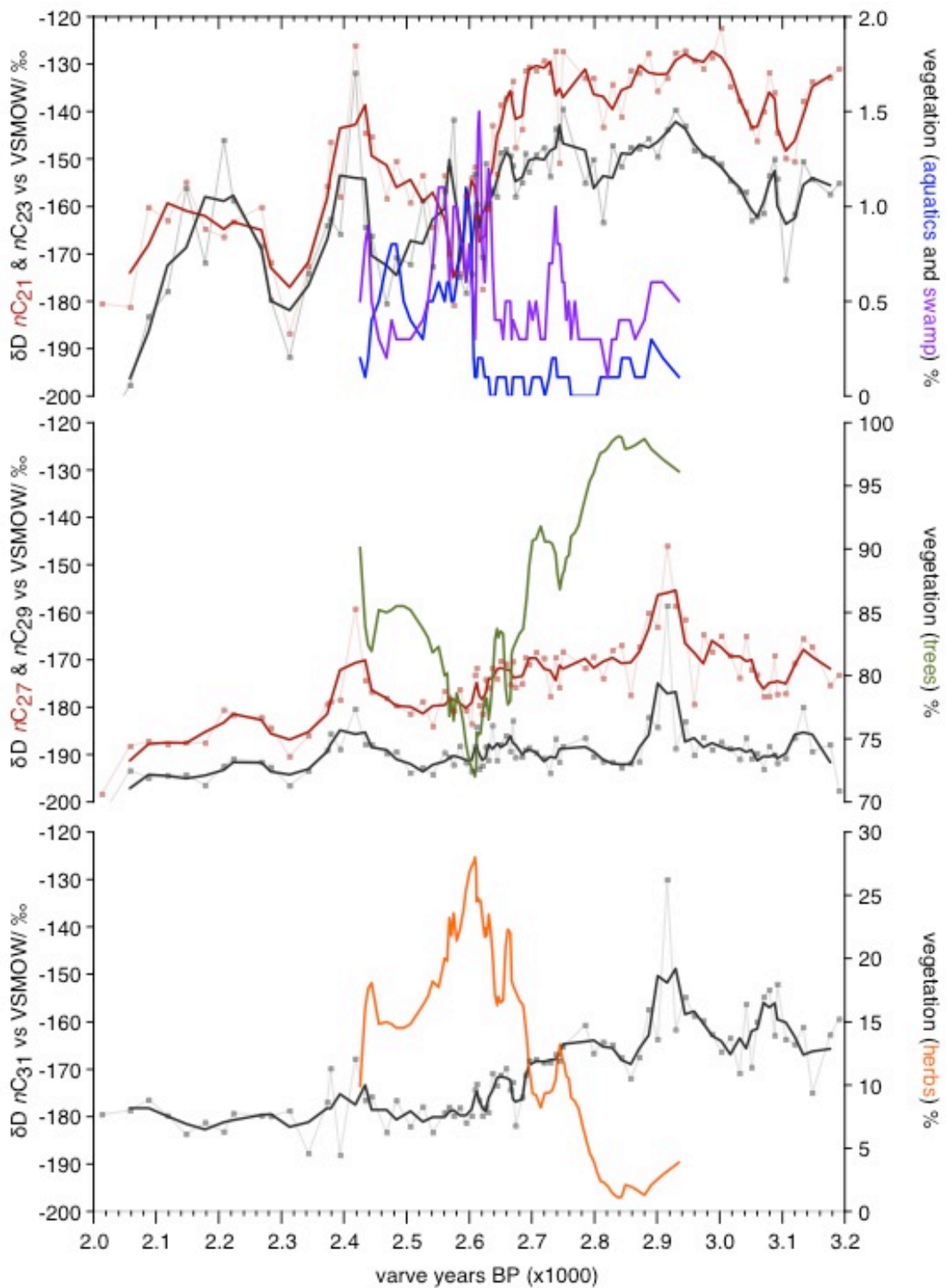
651 *6.2.4. The effect of vegetation changes on δD values of terrestrial n -alkanes*

652 δD values of the terrestrial plant derived nC_{27} , nC_{29} and nC_{31} n -alkanes
653 decreased in total by 15, 4 and 20‰, respectively, during the HCO interval
654 (difference between mean δD values from before and after the HCO) (Fig 2).
655 While changes in nC_{27} and nC_{29} δD values were gradual and can be
656 explained by hydroclimatic changes (i.e. cooler and more humid conditions),
657 the first larger and relatively abrupt decrease within the HCO of about 7‰
658 observed for nC_{31} at 2685 varve years BP coincides with the onset of a 20%
659 increase in grass and other herbaceous pollen (Fig 3) likely caused by an
660 increase of human impact (Kubitz, 2000). As such, the change in δD values of
661 nC_{31} may have been amplified by changes in terrestrial vegetation and
662 influenced not only by climatic but also by anthropogenic factors. While nC_{31}
663 is produced by different tree species (e.g. *Betula*, *Acer* (Diefendorf et al.,
664 2011)) it is often found in higher concentrations in grasses (Massimo, 1996).

665 Therefore, the more negative δD values after 2680 varve years BP may
666 reflect at least partly the increased amount of grass-derived nC_{31} into the lake
667 sediment, as n -alkane δD values from grasses are usually found to be more
668 negative (up to 30‰) compared to those from trees (Duan and He, 2011; Hou
669 et al., 2007; Kahmen et al., 2013b; Liu et al., 2006; Sachse et al., 2012).

670 Based on the palynological data we suggest that the nC_{27} and nC_{29} alkanes in
671 the MFM sediments were primarily produced by trees such as *Alnus*, *Betula*,
672 *Salix*, *Fagus*, *Carpinus*, *Ulmus* and *Quercus*, species known to produce the n -
673 alkanes (Diefendorf et al., 2011; Piasentier et al., 2000; Sachse et al., 2006).
674 Interestingly, nC_{29} δD values from the MFM sediments of the analyzed period
675 were on average 18‰ more negative than nC_{27} and nC_{31} δD values. This
676 consistent offset possibly implies a different water source or a different ϵ_{bio} for
677 all or the major nC_{29} source organisms. The pollen record provides evidence
678 for a high proportion of *Alnus* and *Salix* in the catchment area, taxa primarily
679 adapted to wetter areas such as lake shores and riversides (Landolt and
680 Bäumler, 2010; Lauber and Wagner, 2001). *Alnus* and *Salix* have been found
681 to synthesize higher amounts of nC_{29} (Diefendorf et al., 2011; Sachse et al.,
682 2006) and therefore the more negative nC_{29} δD values may be due to the
683 preferred location at the lakeshore within the crater, where higher relative
684 humidity (due to the proximity of the water body) may have resulted in smaller
685 leaf water isotope enrichment (Craig, 1965; Farquhar et al., 2007; Flanagan et
686 al., 1991; Kahmen et al., 2011; Kahmen et al., 2013b).

687 Due to the wide variety of possible sources of the nC_{27} and nC_{29} alkanes, it is
688 likely that these compounds had the highest integrative capacity and the
689 occurrence or disappearance of single species did not significantly affect the
690 sedimentary δD record. As such δD values of these compounds more
691 faithfully recorded the long-term late Holocene hydroclimatic trend to cooler
692 and wetter conditions. Nevertheless, while less susceptible to changes than
693 species-poor assemblages, major environmental perturbances such as
694 human impact on vegetation, wildfires, etc, can significantly affect diverse and
695 species-rich plant assemblages to the extent that n -alkane records (and their
696 stable isotope records) can be affected.



697

698 **Fig. 4:** Aquatic and terrestrial plant derived sedimentary *n*-alkane δ D record
 699 combined with reconstructed vegetation distribution. Vegetation data shown
 700 as moving average over 3 data points. **(A)** Aquatic plant derived *n*-alkane δ D
 701 records (*n*C₂₁, *n*C₂₃) vs. vegetation population of aquatic and swamp taxa. **(B)**
 702 Terrestrial plant (tree) derived *n*-alkane δ D records (*n*C₂₇, *n*C₂₉) vs. tree

703 population. **(C)** Terrestrial plant (herbs) derived *n*-alkane δD record (nC_{31}) vs.
704 herb population.

705

706 **7. Conclusions**

707 Our combined high-resolution hydroclimate and vegetation study based on
708 lipid biomarker δD and palynological records from lake MFM provides detailed
709 insights into the succession of climate and ecosystem change and
710 emphasizes the advantages of a multiproxy approach for hydroclimate
711 reconstructions during periods of ecological change. Specifically, our results
712 indicate that:

713 (1) Between 3200 and 2000 varve years BP decreasing lipid biomarker δD
714 values reflect the overall late Holocene trend to cooler and/ or wetter
715 conditions.

716 (2) Since lipid biomarker δD values remain more negative after the HCO,
717 we suggest that this period does not only constitute a temporal climatic
718 oscillation triggered by a grand solar minimum, but marks a transition
719 phase resulting in the permanent establishment of cooler and wetter
720 conditions and/or different atmospheric moisture pathways.

721 (3) Our data show that the local aquatic ecosystem composition did
722 change significantly at 2640 varve years BP, ca. 60 years after the
723 onset of changes in the terrestrial ecosystem. This is possibly induced
724 by increased nutrient input due to enhanced soil erosion, which in turn
725 was related to a decrease in vegetation caused by forest clearance.

726 (4) We argue that changes in the source organisms of aquatic *n*-alkanes
727 (possibly associated with different degrees of biosynthetic hydrogen
728 isotope fractionation) at the time of major (aquatic) ecosystem change
729 caused significant changes in δD_{aq} values. Therefore, the appearance
730 and/or disappearance of a single species can result in significant
731 variations in sedimentary δD_{aq} , in particular for lake systems with a
732 limited number of aquatic *n*-alkane source organisms. However, while
733 *n*-alkane spectra of species-poor assemblages might be more
734 susceptible to taxonomic turnover, even changes in species-rich

735 assemblages could significantly affect the *n*-alkane record. As such,
736 changes in the aquatic lipid biomarker δD values during the study
737 period do not only reflect hydroclimate changes but also reflect
738 ecological change, in our case amplifying the climatic signal.

739 (5) In contrast, terrestrial higher plant derived leaf wax *n*-alkanes,
740 produced by a number of different broadleaved tree species and
741 derived from thousands of individual trees in the lake catchment, record
742 an integrated signal of the terrestrial vegetation and, therefore a more
743 reliable hydroclimate record.

744 Our data suggest the importance to consider the different integrative
745 capacities of source specific vs. less specific lipid biomarkers and show that
746 the combination with microfossil records can provide detailed insights into the
747 succession of climatic and ecosystem changes in the lake catchment.

749 **Acknowledgements**

750

751 This work was supported by a DFG Emmy-Noether grant to DS (SA1889/1-1).
752 It is a contribution to the INTIMATE project, which is funded as an EU COST
753 Action and to the Helmholtz Association (HGF) Climate Initiative "REKLIM"
754 Topic 8 'Rapid climate change derived from proxy data' and has used
755 infrastructure of the HGF TERENO programme. Laboratory assistance was
756 provided by Nikolas Werner (UP).

758 **Author contributions**

759 O. Rach carried out the *n*-alkane extraction, analysis, stable isotope
760 measurement, isotope data evaluation and wrote the paper. S. Engels and B.
761 van Geel carried out the pollen analysis, pollen data evaluation and wrote the
762 paper. A. Kahmen provided infrastructure for isotope measurement,
763 contributed to the analysis, data evaluation and writing. A. Brauer was
764 responsible for lake coring, data evaluation and writing. C. Martín-Puertas
765 provided the chronology and stratigraphy, contributed to data evaluation and

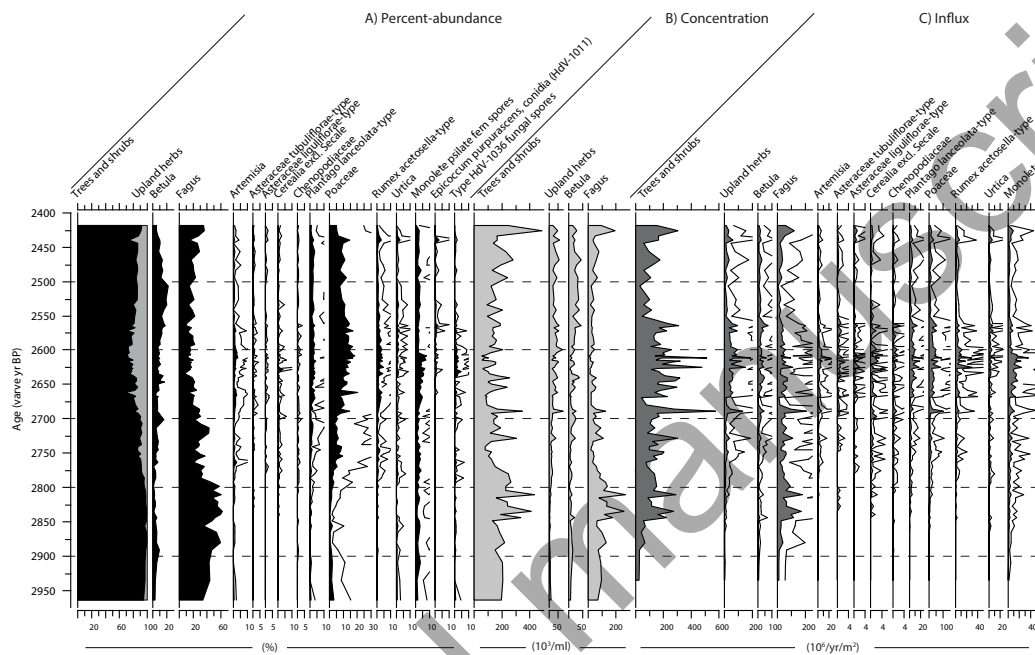
766 wrote the paper. Dirk Sachse conceived the research, acquired financial
767 support and wrote the paper.

768

769 Supplementary information

770

771



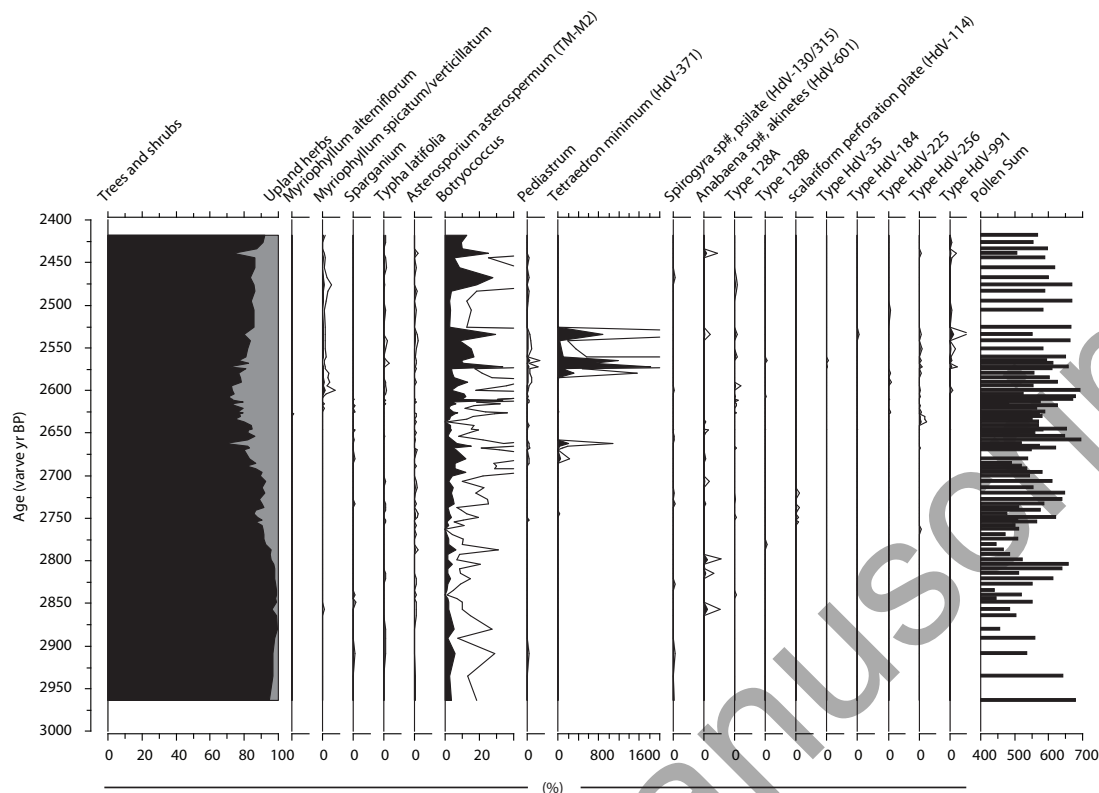
772

773 **Fig. S1:** Overview diagram on arboreal taxa (in percent - left, concentration -
774 middle, influx - right)

775

776

777



778

779 **Fig. S2:** Overview diagram on aquatic taxa (right part) and trees/ shrubs vs.
 780 herbaceous taxa distribution (left) in percent

781

782 References

783

784 Aichner, B., Herzsuh, U., Wilkes, H., Vieth, A., Böhner, J., 2010. δD values of n-
 785 alkanes in Tibetan lake sediments and aquatic macrophytes - A surface sediment
 786 study and application to a 16 ka record from Lake Koucha. *Organic Geochemistry*
 787 41, 779-790.

788 Atwood, A.R., Sachs, J.P., 2014. Separating ITCZ- and ENSO-related rainfall
 789 changes in the Galápagos over the last 3 kyr using D/H ratios of multiple lipid
 790 biomarkers. *Earth and Planetary Science Letters* 404, 408-419.

791 Baas, M., Pancost, R., van Geel, B., Sinninghe Damsté, J.S., 2000. A comparative
 792 study of lipids in *Sphagnum* species. *Organic Geochemistry* 31, 535-541.

793 Baldini, L.M., McDermott, F., Foley, A.M., Baldini, J.U.L., 2008. Spatial variability in
 794 the European winter precipitation $\delta^{18}O$ -NAO relationship: Implications for
 795 reconstructing NAO-mode climate variability in the Holocene. *Geophysical*
 796 *Research Letters* 35, L04709.

- 797 Behre, K.-E., 1981. The interpretation of anthropogenic indicators in pollen
798 diagrams. *Pollen et spores* 23, 225-245.
- 799 Beug, H.J., 2004. Leitfaden der Pollenbestimmung für Mitteleuropa und
800 angrenzende Gebiete. Verlag Dr. Friedrich Pfeil.
- 801 Brauer, A., Endres, C., Günter, C., Litt, T., Stebich, M., Negendank, J.F.W., 1999a.
802 High resolution sediment and vegetation responses to Younger Dryas climate
803 change in varved lake sediments from Meerfelder Maar, Germany. *Quaternary*
804 *Science Reviews* 18, 321-329.
- 805 Brauer, A., Endres, C., Negendank, J.F.W., 1999b. Lateglacial calendar year
806 chronology based on annually laminated sediments from Lake Meerfelder Maar,
807 Germany. *Quaternary International* 61, 17-25.
- 808 Brauer, A., Endres, C., Zolitschka, B., Negendank, J.F.W., 2000. AMS Radiocarbon
809 and varve chronology from the annually laminated sediment record of lake
810 Meerfelder Maar, Germany. *Radiocarbon* 42, 355-368.
- 811 Brauer, A., Haug, G.H., Dulski, P., Sigman, D.M., Negendank, J.F.W., 2008. An
812 abrupt wind shift in western Europe at the onset of the Younger Dryas cold
813 period. *Nature Geoscience* 1, 520-523.
- 814 Craig, G.L., 1965. Deuterium and oxygen 18 variations in the ocean and the
815 marine atmosphere, in: Tongiorgi, E. (Ed.), *Stable Isotopes in Oceanographic*
816 *Studies and Paleotemperatures*. CNR Lab. Geol. Nucl., Pisa, pp. 9–130.
- 817 Cranwell, P.A., Eglinton, G., Robinson, N., 1987. Lipids of aquatic organisms as
818 potential contributors to lacustrine sediments-II. *Organic Geochemistry* 11, 513-
819 527.
- 820 Dansgaard, W., 1964. Stable isotopes in precipitation. *Tellus* 16, 436-468.
- 821 Diefendorf, A.F., Freeman, K.H., Wing, S.L., Graham, H.V., 2011. Production of n-
822 alkyl lipids in living plants and implications for the geologic past. *Geochimica et*
823 *Cosmochimica Acta* 75, 7472-7485.
- 824 Duan, Y., He, J.X., 2011. Distribution and isotopic composition of n-alkanes from
825 grass, reed and tree leaves along a latitudinal gradient in China. *Geochemical*
826 *Journal* 45, 199-207.
- 827 Eglinton, G., Hamilton, R.J., 1967. Leaf epicuticular waxes. *Science* 156, 1322-
828 1327.
- 829 Eglinton, T.I., Eglinton, G., 2008. Molecular proxies for paleoclimatology. *Earth*
830 *and Planetary Science Letters* 275, 1-16.

- 831 Engels, S., Bakker, M., Bohncke, S., Cerli, C., Hoek, W., Jansen, B., Peters, T.,
832 Renssen, H., Sachse, D., Aken, J.v., Bos, V.v.d., Geel, B.v., Oostrom, R.v., Winkels, T.,
833 Wolma, M., 2016a. Centennial-scale lake-level lowstand at Lake Uddelermeer
834 (The Netherlands) indicates changes in moisture source region prior to the 2.8-
835 kyr event. *The Holocene* 26, 1075-1091.
- 836 Engels, S., Brauer, A., Buddelmeijer, N., Martín-Puertas, C., Rach, O., Sachse, D.,
837 van Geel, B., 2016b. Subdecadal-scale vegetation responses to a previously
838 unknown late-Allerød climate fluctuation and Younger Dryas cooling at Lake
839 Meerfelder Maar (Germany). *Journal of Quaternary Science* 31, 741-752.
- 840 Faegri, K., Iversen, J., Kaland, P.E., Krzywinski, K., 1990. Textbook of pollen
841 analysis, 4 ed. John Wiley & Sons, Ltd, Chichester.
- 842 Farquhar, G.D., Cernusak, L.A., Barnes, B., 2007. Heavy water fractionation during
843 transpiration. *Plant Physiol.* 143, 11-18.
- 844 Feakins, S.J., Kirby, M.E., Cheetham, M.I., Ibarra, Y., Zimmerman, S.R.H., 2014.
845 Fluctuation in leaf wax D/H ratio from a southern California lake records
846 significant variability in isotopes in precipitation during the late Holocene.
847 *Organic Geochemistry* 66, 48-59.
- 848 Ficken, K.J., Li, B., Swain, D.L., Eglinton, G., 2000. An n-alkane proxy for the
849 sedimentary input of submerged/floating freshwater aquatic macrophytes.
850 *Organic Geochemistry* 31, 745-749.
- 851 Flanagan, L.B., Comstock, J.P., Ehleringer, J.R., 1991. Comparison of modeled and
852 observed environmental influences on the stable oxygen and hydrogen isotope
853 composition of leaf water in *Phaseolus vulgaris*. *Plant Physiol.* 96, 588-596.
- 854 Gao, L., Edwards, E.J., Zeng, Y.B., Huang, Y.S., 2014. Major Evolutionary Trends in
855 Hydrogen Isotope Fractionation of Vascular Plant Leaf Waxes. *Plos One* 9.
- 856 Gao, L., Hou, J., Toney, J., MacDonald, D., Huang, Y., 2011. Mathematical modeling
857 of the aquatic macrophyte inputs of mid-chain n-alkyl lipids to lake sediments:
858 Implications for interpreting compound specific hydrogen isotopic records.
859 *Geochimica et Cosmochimica Acta* 75, 3781-3791.
- 860 Garcin, Y., Schwab, V.F., Gleixner, G., Kahmen, A., Todou, G., Sene, O., Onana, J.M.,
861 Achoundong, G., Sachse, D., 2012. Hydrogen isotope ratios of lacustrine
862 sedimentary n-alkanes as proxies of tropical African hydrology: Insights from a
863 calibration transect across Cameroon. *Geochimica et Cosmochimica Acta* 79,
864 106-126.
- 865 Gat, J.R., 1996. Oxygen and Hydrogen isotopes in the hydrologic cycle. *Annual*
866 *Review of Earth and Planetary Sciences* 24, 225-262.

- 867 Gat, J.R., Mook, W.G., Meijer, H.A.J., 2000. Environmental Isotopes in
868 the Hydrological Cycle - Principles and Applications - Volume 2: Atmospheric
869 Water, Atmospheric Water. International Atomic Energy Agency and United
870 Nations Educational, Scientific and Cultural Organization, Paris Vienna.
- 871 Gelpi, E., Schneider, H., Mann, J., Oro, J., 1970. Hydrocarbons of geochemical
872 significance in microscopic algae. *Phytochemistry* 9, 603-612.
- 873 Hou, J., D'Andrea, W.J., MacDonald, D., Huang, Y., 2007. Hydrogen isotopic
874 variability in leaf waxes among terrestrial and aquatic plants around Blood Pond,
875 Massachusetts (USA). *Organic Geochemistry* 38, 977-984.
- 876 Huang, Y., Shuman, B., Wang, Y., Webb, T., 2004. Hydrogen isotope ratios of
877 individual lipids in lake sediments as novel tracers of climatic and environmental
878 change: a surface sediment test. *Journal of Paleolimnology* 31, 363-375.
- 879 IAEA/WMO, 2006. Global Network of Isotopes in Precipitation. The GNIP
880 Database, Bundesanstalt fuer Gewaesserkunde.
- 881 Kahmen, A., Hoffmann, B., Schefuss, E., Arndt, S.K., Cernusak, L.A., West, J.B.,
882 Sachse, D., 2013a. Leaf water deuterium enrichment shapes leaf wax n-alkane
883 delta D values of angiosperm plants II: Observational evidence and global
884 implications. *Geochimica et Cosmochimica Acta* 111, 50-63.
- 885 Kahmen, A., Sachse, D., Arndt, S.K., Tu, K.P., Farrington, H., Vitousek, P.M.,
886 Dawson, T.E., 2011. Cellulose delta(18)O is an index of leaf-to-air vapor pressure
887 difference (VPD) in tropical plants. *Proceedings of the National Academy of
888 Sciences* 108, 1981-1986.
- 889 Kahmen, A., Schefuss, E., Sachse, D., 2013b. Leaf water deuterium enrichment
890 shapes leaf wax n-alkane delta D values of angiosperm plants I: Experimental
891 evidence and mechanistic insights. *Geochimica et Cosmochimica Acta* 111, 39-49.
- 892 Killops, S., Killops, V., 2005. Introduction to organic geochemistry, 2nd ed.
893 Blackwell Publishing, Malden (USA), Oxford (UK), Carlton (Australia).
- 894 Kubitz, B., 2000. History of Holocene vegetation and human settlement in
895 Western Eifel (Germany) based on a high-resolution pollen diagram from the
896 Meerfelder Maar Lake, [Dissertationes Botanicae. History of Holocene vegetation
897 and human settlement in Western Eifel. J. Cramer in der Gebrueder Borntraeger
898 Verlagsbuchhandlung, D-14129, Berlin, Germany, pp. 1-106.
- 899 Landolt, E., Bäuml, B., 2010. Flora indicativa: ökologische Zeigerwerte und
900 biologische Kennzeichen zur Flora der Schweiz und der Alpen. Ed. des
901 Conservatoire et Jardin botaniques de la ville de Genève.

- 902 Lauber, K., Wagner, G., 2001. Flora Helvetica, 3. Auflage ed. Verlag Paul Haupt,
903 Bern; Stuttgart; Wien.
- 904 Litt, T., Brauer, A., Goslar, T., Merkt, J., Balaga, K., Müller, H., Ralska-Jasiewiczowa,
905 M., Stebich, M., Negendank, J.F.W., 2001. Correlation and synchronisation of
906 Lateglacial continental sequences in northern central Europe based on annually
907 laminated lacustrine sediments. *Quaternary Science Reviews* 20, 1233-1249.
- 908 Litt, T., Scholzel, C., Kuhl, N., Brauer, A., 2009. Vegetation and climate history in
909 the Westeifel Volcanic Field (Germany) during the past 11000 years based on
910 annually laminated lacustrine maar sediments. *Boreas* 38, 679-690.
- 911 Liu, W.G., Yang, H., Li, L.W., 2006. Hydrogen isotopic compositions of n-alkanes
912 from terrestrial plants correlate with their ecological life forms. *Oecologia* 150,
913 330-338.
- 914 Magny, M., 1993. Solar influences on Holocene climate changes illustrated by
915 correlations between past lake-level fluctuations and the atmospheric C14
916 record. *Quaternary Research* 40, 1-9.
- 917 Marcott, S.A., Shakun, J.D., Clark, P.U., Mix, A.C., 2013. A Reconstruction of
918 Regional and Global Temperature for the Past 11,300 Years. *Science* 339, 1198-
919 1201.
- 920 Martin-Puertas, C., Brauer, A., Dulski, P., Brademann, B., 2012a. Testing climate-
921 proxy stationarity throughout the Holocene: an example from the varved
922 sediments of Lake Meerfelder Maar (Germany). *Quaternary Science Reviews* 58,
923 56-65.
- 924 Martin-Puertas, C., Matthes, K., Brauer, A., Muscheler, R., Hansen, F., Petrick, C.,
925 Aldahan, A., Possnert, G., van Geel, B., 2012b. Regional atmospheric circulation
926 shifts induced by a grand solar minimum. *Nature Geoscience* 5, 397-401.
- 927 Massimo, M., 1996. Chemotaxonomic significance of leaf wax alkanes in the
928 Gramineae. *Biochemical Systematics and Ecology* 24, 53-64.
- 929 McInerney, F.A., Helliker, B.R., Freeman, K.H., 2011. Hydrogen isotope ratios of
930 leaf wax n-alkanes in grasses are insensitive to transpiration. *Geochimica et*
931 *Cosmochimica Acta* 75, 541-554.
- 932 Moore, P.D., Webb, J.A., Collinson, M.E., 1991. Pollen analysis, Second edition.
933 Blackwell Scientific Publications, 3 Cambridge Center, Cambridge, Massachusetts
934 02142, USA Osney Mead, Oxford OX2 0EL, England.

- 935 Moschen, R., Lucke, A., Schleser, G.H., 2005. Sensitivity of biogenic silica oxygen
936 isotopes to changes in surface water temperature and palaeoclimatology.
937 *Geophysical Research Letters* 32.
- 938 Movius, H.L., 2013. *The Irish Stone Age*. Cambridge University Press.
- 939 Nelson, D.M., Henderson, A.K., Huang, Y.S., Hu, F.S., 2013. Influence of terrestrial
940 vegetation on leaf wax delta D of Holocene lake sediments. *Organic Geochemistry*
941 56, 106-110.
- 942 Parrish, C.C., 1988. Dissolved and particulate marine lipid classes - a review.
943 *Marine Chemistry* 23, 17-40.
- 944 Peters, K.E., Moldowan, J.M., Walters, C.C., 2007. *The Biomarker Guide: Volume 1,*
945 *Biomarkers and Isotopes in the Environment and Human History*. Cambridge
946 University Press.
- 947 Piasentier, E., Bovolenta, S., Malossini, F., 2000. The n-alkane concentrations in
948 buds and leaves of browsed broadleaf trees. *Journal of Agricultural Science* 135,
949 311-320.
- 950 Rach, O., Brauer, A., Wilkes, H., Sachse, D., 2014. Delayed hydrological response to
951 Greenland cooling at the onset of the Younger Dryas in western Europe. *Nature*
952 *Geoscience* 7, 109-112.
- 953 Reimer, P.J., Baillie, M.G.L., Bard, E., Bayliss, A., Beck, J.W., Blackwell, P.G., Ramsey,
954 C.B., Buck, C.E., Burr, G.S., Edwards, R.L., Friedrich, M., Grootes, P.M., Guilderson,
955 T.P., Hajdas, I., Heaton, T.J., Hogg, A.G., Hughen, K.A., Kaiser, K.F., Kromer, B.,
956 McCormac, F.G., Manning, S.W., Reimer, R.W., Richards, D.A., Southon, J.R.,
957 Talamo, S., Turney, C.S.M., van der Plicht, J., Weyhenmeyer, C.E., 2009. Intcal09
958 and Marine09 radiocarbon age calibration curves, 0-50,000 years cal BP.
959 *Radiocarbon* 51, 1111-1150.
- 960 Renssen, H., Seppä, H., Heiri, O., Roche, D.M., Goosse, H., Fichefet, T., 2009. The
961 spatial and temporal complexity of the Holocene thermal maximum. *Nature*
962 *Geoscience* 2, 410-413.
- 963 Sachs, J.P., 2014. Hydrogen Isotope Signatures in the Lipids of Phytoplankton, in:
964 Holland, H.D., Turekian, K.K. (Eds.), *Treatise on Geochemistry*, Second Edition ed.
965 Elsevier, Oxford, pp. 79-94.
- 966 Sachs, J.P., Pahnke, K., Smittenberg, R., Zhang, Z., 2013. Biomarker Indicators of
967 Past Climate, in: Mock, S.A.E.J. (Ed.), *Encyclopedia of Quaternary Science* (Second
968 Edition). Elsevier, Amsterdam, pp. 775-782.

- 969 Sachs, J.P., Sachse, D., Smittenberg, R.H., Zhang, Z.H., Battisti, D.S., Golubic, S.,
970 2009. Southward movement of the Pacific intertropical convergence zone AD
971 1400-1850. *Nature Geoscience* 2, 519-525.
- 972 Sachse, D., Billault, I., Bowen, G.J., Chikaraishi, Y., Dawson, T.E., Feakins, S.J.,
973 Freeman, K.H., Magill, C.R., McInerney, F.A., van der Meer, M.T.J., Polissar, P.,
974 Robins, R.J., Sachs, J.P., Schmidt, H.-L., Sessions, A.L., White, J.W.C., West, J.B.,
975 Kahmen, A., 2012. Molecular Paleohydrology: Interpreting the Hydrogen-
976 Isotopic Composition of Lipid Biomarkers from Photosynthesizing Organisms.
977 *Annual Review of Earth and Planetary Sciences* 40, 221-249.
- 978 Sachse, D., Radke, J., Gleixner, G., 2004. Hydrogen isotope ratios of recent
979 lacustrine sedimentary n-alkanes record modern climate variability. *Geochimica
980 et Cosmochimica Acta* 68, 4877-4889.
- 981 Sachse, D., Radke, J., Gleixner, G., 2006. δD values of individual n-alkanes from
982 terrestrial plants along a climatic gradient - Implications for the sedimentary
983 biomarker record. *Organic Geochemistry* 37, 469-483.
- 984 Sachse, D., Sachs, J.P., 2008. Inverse relationship between D/H fractionation in
985 cyanobacterial lipids and salinity in Christmas Island saline ponds. *Geochimica et
986 Cosmochimica Acta* 72, 793-806.
- 987 Sauer, P.E., Eglinton, T.I., Hayes, J.M., Schimmelmann, A., Sessions, A.L., 2001.
988 Compound-specific D/H ratios of lipid biomarkers from sediments as a proxy for
989 environmental and climatic conditions. *Geochimica et Cosmochimica Acta* 65,
990 213-222.
- 991 Schefuss, E., Kuhlmann, H., Mollenhauer, G., Prange, M., Pätzold, J., 2011. Forcing
992 of wet phases in southeast Africa over the past 17,000 years. *Nature* 480, 509-
993 512.
- 994 Scott, E.M., Alekseev, A.Y., Zaitseva, G., 2006. Impact of the Environment on
995 Human Migration in Eurasia: Proceedings of the NATO Advanced Research
996 Workshop, held in St. Petersburg, 15-18 November 2003. Springer Netherlands.
- 997 Sessions, A.L., Burgoyne, T.W., Schimmelmann, A., Hayes, J.M., 1999.
998 Fractionation of hydrogen isotopes in lipid biosynthesis. *Organic Geochemistry*
999 30, 1193-1200.
- 1000 Sessions, A.L., Hayes, J.M., 2005. Calculation of hydrogen isotopic fractionations
1001 in biogeochemical systems. *Geochimica et Cosmochimica Acta* 69, 593-597.
- 1002 Smittenberg, R.H., Saenger, C., Dawson, M.N., Sachs, J.P., 2011. Compound-specific
1003 D/H ratios of the marine lakes of Palau as proxies for West Pacific Warm Pool
1004 hydrologic variability. *Quaternary Science Reviews* 30, 921-933.

- 1005 Stockmarr, J., 1971. Tablets with spores used in absolute pollen analysis. *Pollen*
1006 *et Spores* 13, 615-621.
- 1007 Swierczynski, T., Lauterbach, S., Dulski, P., Delgado, J., Merz, B., Brauer, A., 2013.
1008 Mid- to late Holocene flood frequency changes in the northeastern Alps as
1009 recorded in varved sediments of Lake Mondsee (Upper Austria). *Quaternary*
1010 *Science Reviews* 80, 78-90.
- 1011 Tierney, J.E., Oppo, D.W., Rosenthal, Y., Russell, J.M., Linsley, B.K., 2010.
1012 Coordinated hydrological regimes in the Indo-Pacific region during the past two
1013 millennia. *Paleoceanography* 25.
- 1014 Tierney, J.E., Russell, J.M., Huang, Y.S., Sinninghe Damsté, J.S., Hopmans, E.C.,
1015 Cohen, A.S., 2008. Northern hemisphere controls on tropical southeast African
1016 climate during the past 60,000 years. *Science* 322, 252-255.
- 1017 Van Geel, B., 1978. A palaeoecological study of holocene peat bog sections in
1018 Germany and The Netherlands, based on the analysis of pollen, spores and
1019 macro- and microscopic remains of fungi, algae, cormophytes and animals.
1020 *Review of Palaeobotany and Palynology* 25, 1-120.
- 1021 van Geel, B., Berglund, B.E., 2000. A causal link between a climatic deterioration
1022 around 850 cal BC and a subsequent rise in human population density in NW-
1023 Europe? *Terra Nostra* 7, 126-130.
- 1024 van Geel, B., Buurman, J., Waterbolk, H.T., 1996. Archaeological and
1025 palaeoecological indications of an abrupt climate change in The Netherlands, and
1026 evidence for climatological teleconnections around 2650 BP. *Journal of*
1027 *Quaternary Science* 11, 451-460.
- 1028 van Geel, B., Engels, S., Martin-Puertas, C., Brauer, A., 2013. Ascospores of the
1029 parasitic fungus *Kretzschmaria deusta* as rainstorm indicators during a late
1030 Holocene beech-forest phase around lake Meerfelder Maar, Germany. *Journal of*
1031 *Paleolimnology* 50, 33-40.
- 1032 van Geel, B., Raspopov, O.M., Renssen, H., van der Plicht, J., Dergachev, V.A.,
1033 Meijer, H.A.J., 1999. The role of solar forcing upon climate change. *Quaternary*
1034 *Science Reviews* 18, 331-338.
- 1035 Vonmoos, M., Beer, J., Muscheler, R., 2006. Large variations in Holocene solar
1036 activity: Constraints from Be-10 in the Greenland Ice Core Project ice core.
1037 *Journal of Geophysical Research-Space Physics* 111.
- 1038 Wanner, H., Beer, J., Butikofer, J., Crowley, T.J., Cubasch, U., Fluckiger, J., Goosse,
1039 H., Grosjean, M., Joos, F., Kaplan, J.O., Kuttel, M., Muller, S.A., Prentice, I.C.,
1040 Solomina, O., Stocker, T.F., Tarasov, P., Wagner, M., Widmann, M., 2008. Mid- to

- 1041 Late Holocene climate change: an overview. *Quaternary Science Reviews* 27,
1042 1791-1828.
- 1043 Wirth, S.B., Glur, L., Gilli, A., Anselmetti, F.S., 2013. Holocene flood frequency
1044 across the Central Alps – solar forcing and evidence for variations in North
1045 Atlantic atmospheric circulation. *Quaternary Science Reviews* 80, 112-128.
- 1046 Zhang, Z., Leduc, G., Sachs, J.P., 2014. El Niño evolution during the Holocene
1047 revealed by a biomarker rain gauge in the Galápagos Islands. *Earth and Planetary
1048 Science Letters* 404, 420-434.
- 1049 Zhang, Z., Sachs, J.P., 2007. Hydrogen isotope fractionation in freshwater algae: I.
1050 Variations among lipids and species. *Organic Geochemistry* 38, 582-608.
- 1051 Zolitschka, B., Brauer, A., Negendank, J.F.W., Stockhausen, H., Lang, A., 2000.
1052 Annually dated late Weichselian continental paleoclimate record from the Eifel,
1053 Germany. *Geology* 28, 783-786.
- 1054 Zöller, L., Blanchard, H., 2009. The partial heat – longest plateau technique:
1055 Testing TL dating of Middle and Upper Quaternary volcanic eruptions in the Eifel
1056 Area, Germany. *E&G - Quaternary Science Journal* 58, p. 86-107.
1057
1058